Black Sea Journal of Engineering and Science
doi: 10.34248/bsengineering.1557319

Open Access Journal
e-ISSN: 2619 – 8991

Research Article
Volume 8 - Issue 1: 1-10 / January 2025

EFFECTS OF LOADING TYPE AND LOADING RATE ON GLULAM SIPO TIMBER BEAMS FOR FLEXURAL LOADING

Minel Ahu KARA ALAŞALVAR[1]*

[1]*Gazi University, Graduate School of Natural and Applied Sciences, 06500, Ankara, Türkiye*

Abstract: Glulam wood elements are a high-performance structural material created by bonding layers of wood with structural adhesives. This study investigates the behavior of glulam beams made from the tropical timber species Sipo, which has limited representation in existing literature, under different loading types and rates in bending tests. Six Sipo glulam beams were tested: three under four-point bending and three under three-point bending. To assess the behavior at various loading rates, loads were applied at rates of 10 mm/min, 20 mm/min, and 30 mm/min. The results included load-displacement curves, ultimate load capacities, initial stiffness, and energy dissipation capacities. The study revealed differences between values obtained from three-point and four-point bending tests. Generally, beams subjected to three-point bending yielded higher values than those tested under four-point bending at the same loading rates. Notably, a significant reduction in values was observed for both testing methods at the loading rate of 20 mm/min.

Keywords: Glulam, Bending tests, Strength, Tropical timber

***Corresponding author:** Gazi University, Graduate School of Natural and Applied Sciences, 06500, Ankara, Türkiye
E mail: minelahukara@gmail.com (M. A. KARA ALAŞALVAR)
Minel Ahu KARA ALAŞALVAR https://orcid.org/0000-0003-1138-1446

Received: September 27, 2024
Accepted: November 15, 2024
Published: January 15, 2025

Cite as: Kara Alaşalvar MA. 2025. Effects of loading type and loading rate on glulam sipo timber beams for flexural loading. BSJ Eng Sci, 8(1): 1-10.

1. Introduction

Wood has long been one of the natural and renewable materials used in construction. Over the centuries, the use of wood has been observed in various structures, including wooden houses, bridges, waterfront structures, and utility poles. The simplicity of production, lightweight nature, reusability, and environmental compatibility of wood make it a preferred material for lightweight structures. With the advancement of technology, wood continues to maintain its importance today. Modern technological innovations have enhanced the durability of wood, leading to the emergence of many new wood products such as plywood, particleboard, and other panel products. The glue-lamination process has significantly improved dimensional and surface laminations in wood, resulting in increased load-carrying capacity (Issa and Kmeid, 2005).

One of the oldest engineered wood products is glulam. Glulam is an engineering product created by laminating two or more layers of wood boards in parallel to the direction of the fibers. Compared to other building materials, glulam offers significant advantages. First, it allows for the production of large and wide components, making it possible to obtain long elements even from small trees, which is particularly beneficial for structural elements spanning wide spaces. Another advantage lies in architectural design; the production process allows for the creation of various architectural elements that would be challenging to achieve with other materials due to the bending of the wood. Additionally, the drying of the timber before production minimizes potential drying defects. One of the most important benefits of glulam is the ability to produce variable cross-sections. In glulam beams, large quantities of lower-quality timber can be used in the laminated sections that experience less stress. Generally, higher-grade laminations are positioned near the upper and lower edges of the beams, where higher stresses occur, while lower-grade laminations are utilized in the interior sections of the beams (toward the center). Furthermore, different species can be selected to meet the structural requirements of the laminations (Stark et al., 2010).

Glulam technology enables the production of various structural elements, including bending, axial, curved, and tapered straight members (Stark et al., 2010). Notably, recent studies in the literature focus on glulam beams. Wang et al. (2024) investigated the reinforcement of glulam beams with epoxy resin-bonded prestressing tendons, analyzing the effects of prestressing force levels and bonded types on the flexural behavior of these beams. The study involved four-point bending tests on 12 beams prepared using unreinforced, unbonded, or bonded prestressing techniques, revealing a significant increase of up to 78.8% in flexural capacity and 13.5% in stiffness compared to unreinforced beams (Wang et al., 2024). Das et al. (2023) explored the applicability of the Albizia procera species in glulam beam production, finding its physical and mechanical properties superior

to those of solid Albizia procera timber (Das et al., 2023). Li et al. (2024) discuss the limitations in load-bearing capacity and stiffness of beam joints in long-span wooden structural elements that are joined using self-drilling screws. To address these limitations, they propose inclined self-drilling screw connections made from engineered bamboo. High strength engineered bamboo plates were employed to enhance the joints of the glued laminated timber (glulam) beams. Within the scope of the experimental study, 13 glulam beams were designed, and four-point bending tests were conducted on the samples. The results indicated that the mechanical properties of beams connected with parallel self-drilling screws were superior to those connected with staggered self-drilling screws. Additionally, it was found that the bending capacity of glulam beams combined with parallel-engineered bamboo scrimber plates increased with the number of self-drilling screws used (Li et al., 2024). Zhang et al. (2023) proposed a design for a hollow rectangular cross-section glulam beam with high bending behavior and stability. To enhance the load-bearing capacity, the beam's bottom was reinforced with fiber reinforced polymer (FRP elements). The study investigated the bending behavior of the beam through experimental, theoretical, and finite element methods. The results showed that the reinforced Glulam beams exhibited increased load-bearing capacity, and that the strengthening effect of CFRP elements was superior to that of BFRP elements (Zhang et al., 2023). Mercimek et al. (2024) conducted a four-point bending test on 26 glulam beams to investigate how various factors—including the number of laminated layers, the distance between finger joint connections, the direction of the finger joints, the use or non-use of reinforcement, and the spacing of CFRP strips—affect the bending behavior of glulam beams. The results obtained from the experimental study were compared with numerical analyses conducted using the finite element software ABAQUS. The study concluded that the developed reinforcement method incorporating CFRP strips enhanced the load-bearing capacity of finger-jointed glulam beams and positively influenced the overall load-displacement behavior (Mercimek et al., 2024). Mei et al. (2024) conducted a study on glulam beams reinforced with connected steel rods. The research aimed to evaluate the reinforcement ratio and pre-tensioning level, as well as to assess the impact of unconnected steel rods on the bending capacity of the beams. Theoretical models of both unconnected reinforced and pre-tensioned glulam beams were presented. Consequently, minimum and maximum reinforcement ratios were determined based on beam cracking and variations in sectional stresses. The study also involved relevant analyses to develop a bending capacity prediction model (Mei et al., 2024). İşleyen et al. (2023) investigated the overall behavior of glulam beams reinforced with CFRP strips and the performance of timber under rapid dynamic impact loading in conjunction with reinforcement. In the study, CFRP strip elements were placed in the lower section of the glulam beams and between multiple L-layers of laminated beam components. Additionally, fan-type anchors were applied to delay the separation of CFRP strip elements from the surface. The reinforced glulam elements were compared with reference samples that did not receive reinforcement. The CFRP-reinforced glulam beams were also modeled using ABAQUS finite element software (İşleyen et al., 2023). Wang et al. (2024) conducted a study utilizing birch plywood panels to bond two glulam beam halves for creating a long span. In this study, four-point bending tests were applied to the samples using birch plywood in the mid-span region of the glulam beams. Numerical and analytical modeling were performed, revealing that the developed models aligned well with the obtained test results (Wang et al., 2024). Zhao et al. (2023) conducted a study on a self-balancing system known as a glulam beam series for large-span glulam structures. Five-point bending tests were performed on the prepared samples. The study found that as the diameter increased, the damage mode of the samples changed, ranging from failure of the lower steel cables to damage in the upper glulam beams. Various parameter analyses were considered to develop numerical models, and a series of design recommendations were presented, taking into account both load capacity and economic impacts (Zhao et al., 2023). Yang et al. (2016) conducted an experimental and theoretical study investigating the bending behavior of glulam beams reinforced with FRP and steel elements. In the study, Douglas fir was used, and the test samples were prepared both as reinforced and unreinforced, undergoing four-point bending tests. The effects of reinforcement materials, reinforcement ratios, and configurations on bending behavior were examined. The results indicated that the reinforced beams exhibited improved bending capacity, overall bending stiffness, and tensile deformation at failure compared to the unreinforced control beams (Yang et al., 2016). He et al. (2022) conducted four-point bending tests on 18 glulam wooden beams, either unreinforced or reinforced with CFRP. The study investigated the effects of the elastic modulus of CFRP and the configuration of CFRP on bending performance. The results indicated that the reinforced glulam beams exhibited a more ductile bending failure characteristic compared to the unreinforced beams (He et al., 2022). Uzel et al. (2018) compared the bending behavior of glulam beams made from Pinus sylvestris with that of solid wood beams. The variables considered in the study included the number of laminations, types of adhesives used, and the reinforcement grids applied to the laminated surfaces. The results indicated that the highest ultimate load capacity was observed in beams made with five laminated layers, utilizing polyurethane adhesives and steel wire reinforcement grids (Uzel et al., 2018). İşleyen et al. (2021a) conducted a study on the reinforcement of

laminated timber beams. In this context, they examined glulam beams by determining the variables associated with the application of CFRP strips in different configurations and CFRP fan-type anchors at the ends of the strips. The study involved testing reinforced laminated timber beams, both anchored and unanchored with CFRP strips, using a three-point bending test. The results included load-displacement graphs of the specimens, from which various interpretations were made (İşleyen et al., 2021a). In another study, İşleyen et al. (2021b) experimentally investigated the behavior under bending loads of three-layer laminated timber beams reinforced with CFRP strips, both anchored and unanchored, featuring different adhesive lengths. The findings indicated that increasing the adhesive length of the CFRP strips and employing CFRP fan-type anchors at the strip ends enhanced the ultimate load capacity, initial stiffness values, displacement ductility ratios, and energy dissipation capacity of the timber beams (İşleyen et al., 2021b). Ghoroubi et al. (2022) conducted an experimental study on the general load-displacement behavior, stress distributions, and shear stress-shear displacement behavior in the connection zones where wooden structural elements are bonded with adhesive or mechanical anchors. The experimental work examined the overall load-displacement behavior of wooden connection areas combined with adhesive and mechanical anchors at lengths of 180, 240, and 350 mm. The study proposed a generalized material model for the shear stress-shear displacement interface at wooden-to-wood connection points (Ghoroubi et al., 2022).

Based on the conducted investigations, it has been determined that there are studies on glulam beams in the literature, with recent research increasingly focusing on the reinforcement of glulam beams. Furthermore, in the experimental studies found in the literature, the loading types applied to glulam beams under bending are generally uniform (either three-point or four-point loading), allowing for an examination of the mechanical properties of the glulam beams. Additionally, when reviewing the experimental studies in the literature, it is observed that there are a limited number of studies where both three-point and four-point bending tests are applied together, and most of these studies primarily concentrate on solid wood elements. In recent literature, studies involving both loading types on massive wood elements have been examined. Notably, research by Hein and Brancheriau (2018) focused on Eucalyptus species, while Brancheriau et al. (2002) investigated six different wood types. Additionally, Yoshihara (2013) explored solid wood, MDF, and five-plywood wood elements, and Babiak et al. (2018) analyzed spruce and oak wood samples. In this context, examining the behavior of glulam beams under different loading types during bending tests is crucial for comprehensively evaluating and interpreting their load-displacement behaviors, initial stiffness, and energy dissipation capacities, thereby contributing to the literature. The study investigates the overall load-displacement behavior and other related mechanical properties of glulam beams under various bending loads (three-point and four-point bending) and differentiates loading rates (10 mm/min, 20 mm/min, and 30 mm/min) to experimentally reveal the influence of loading rates on the overall load-displacement graph of the glulam beams.

In this study, six glulam wood beam elements were prepared using Sipo wood species. Three of the glulam beams were subjected to four-point bending tests, while the other three underwent three-point bending tests. Additionally, the specimens were subjected to different loading rates (10 mm/min, 20 mm/min, and 30 mm/min) under a constant load. By comparing the overall behaviors of the specimens under different loading types and rates, the results were interpreted through general load-displacement graphs, ultimate load capacity, displacement at ultimate load, initial stiffness, and energy dissipation capacity values.

2. Materials and Methods

2.1. Test specimens and materials

In the experimental study, laminated wood beam test specimens were produced using Sipo wood through the glulam engineering technique. As part of the testing program, six glulam Sipo wood beam elements were prepared (Table 1). These specimens were tested under three-point and four-point bending loads, which were monotonically increased until failure occurred. The variables examined in this study included loading type and loading rate. The behaviors of the glulam beams under different loading types and rates were characterized through their overall load-displacement graphs. In this context, it is aimed to make a significant contribution to the literature by revealing the general load-displacement behavior, initial stiffness and energy dissipation capacity of the tropical sipo tree species selected in the study and used as a glulam beam, which is included in a few studies in the literature.

Table 1. Properties of test specimens

Specimen	Dimensions (mm)	Number of glulam layer
1 2 3 4 5 6	72 x 90 x 1450	3

The wooden beams were prepared with dimensions of 72 x 90 x 1450 mm. The laminated wooden beams were produced in three layers, each with a thickness of 24 mm. The experimental study utilized the tropical wood species known as Sipo, which has been less frequently studied in the literature. Care was taken to select wood for the experimental work that did not contain defects

such as knots, cracks, or fiber irregularities. The physical and mechanical properties of Sipo wood are presented in Table 2. Furthermore, in the production of Sipo glulam, PVA d3/d4 (polyvinyl acetate) adhesive from the manufacturer *"Follmann"* was used, with attention to ensuring that the materials to be bonded were dry and free of dust and grease. Three wooden elements, each 24 mm thick, were bonded together using polyvinyl acetate adhesive, completing the production of the glulam wooden beams.

Table 2. Physical and mechanical properties of sipo wood (Gérard et al., 2017)

Properties	Value	Unit
Density	0,62	g/cm^3
Coefficient of volumetric shrinkage	0,42%	per %
Crushing strength	56	MPa
Static bending strength	91	MPa
Longitudinal modulus of elasticity	13,240	MPa

Note: at 12% moisture content, with 1MPa=1 N/mm^2

In the experimental study, the four-point bending test setup applied to glulam beams is illustrated in Figure 1, while the three-point bending test setup is shown in Figure 2. The experimental study program for the test specimens is presented in Table 3.

2.2. Bending Test Setup

In the experimental study, bending tests were conducted using a servo-hydraulic loading system of MTS-322 brand with a capacity of 500 kN. A hydraulic actuator system with a capacity of 500 kN was employed to apply loads to the test specimens, and deformations were measured. At this point, the first group of tests, consisting of specimens numbered 1, 2, and 3, underwent four-point bending tests at a constant loading rate; the loading rates were set at 10 mm/min for specimen 1, 20 mm/min for specimen 2, and 30 mm/min for specimen 3. The four-point static bending load was monotonically increased until the specimens failed. In the second group of tests, consisting of specimens numbered 4, 5, and 6, three-point bending tests were similarly conducted at a constant loading rate; the loading rates were 10 mm/min for specimen 4, 20 mm/min for specimen 5, and 30 mm/min for specimen 6. The three-point static bending load was monotonically increased until the specimens failed. The tests were conducted based on load-displacement graphs.

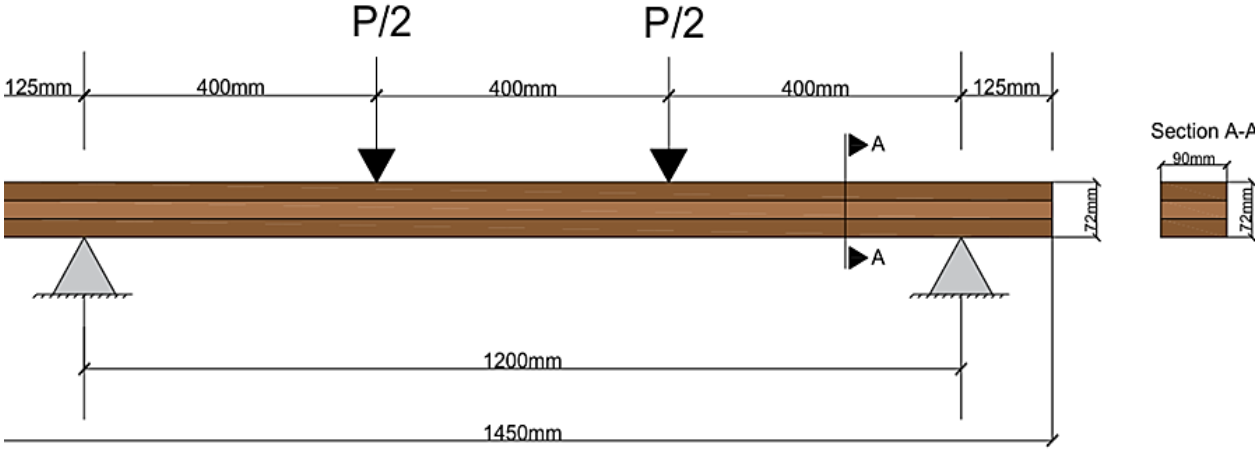

Figure 1. The four-point bending test setup applied to glulam beams.

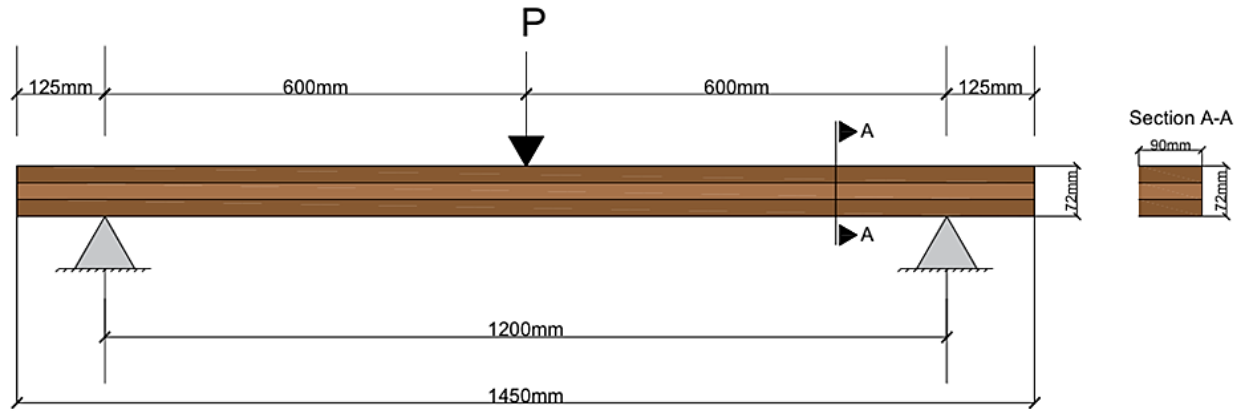

Figure 2. The three-point bending test setup applied to glulam beams.

Table 3. Experimental study program

Specimen	Loading type	Loading rate
1	Four point bending	10 mm/min
2		20 mm/min
3		30 mm/min
4	Three point bending	10 mm/min
5		20 mm/min
6		30 mm/min

3. Results and Discussion

The ultimate load capacity, displacement at ultimate load, initial stiffness, max. displacement, and energy dissipation capacity values were interpreted from the load-displacement graphs of the experimental specimens. The results obtained from the experimental study and the calculated values are presented in Table 4. The test specimens' initial stiffness values were calculated by proportioning the 10 kN load value to the displacement at that point, where no slope change occurred in the load-displacement graphs. It was observed that the ultimate load-bearing capacity of the test specimens decreased by 15%, falling below 85% of their ultimate carrying capacity, which were identified as the failure points of the specimens in the experimental study. The initial stiffness values of the experimental specimens were calculated using the slope of the linear portion of the load-displacement graphs in the initial region. The energy dissipation capacity values were obtained by calculating the area under the load-displacement graphs. In calculating the energy dissipation capacities of the experimental specimens, the area under the graphs was calculated by taking the region up to the point of failure. The points and approaches used in the calculations are illustrated on a typical load-displacement graph in Figure 3. The data obtained from the experimental study are illustrated with graphs and shown in Figure 4. Load-displacement graphs obtained as a result of the experimental study are given in Figure 5. Photographs illustrating the failure states of the specimens after the experimental study are shown in Figure 6.

Table 4. Experimental results

Specimen	Ultimate load capacity(kN)	Displacement at ultimate load (mm)	Initial Stiffness (kN/mm)	Max. displacement (mm)	Energy dissipation capacity (kN.mm)	Failure mode
1	18,27	15,83	1,15	15,84	142,48	Cracking and separation in the tension zone
2	18,13	15,22	1,19	15,23	134,91	Separation and fractures in the tension zone
3	41,12	33,38	1,23	33,41	726,53	Cracking and separation in the tensile zone
4	23,75	36,76	0,65	36,89	508,65	Cracks in the tension zone
5	18,57	28,86	0,64	28,88	288,28	Cracks in the tension zone
6	19,84	21,44	0,93	21,47	214,11	Cracks in the tension zone

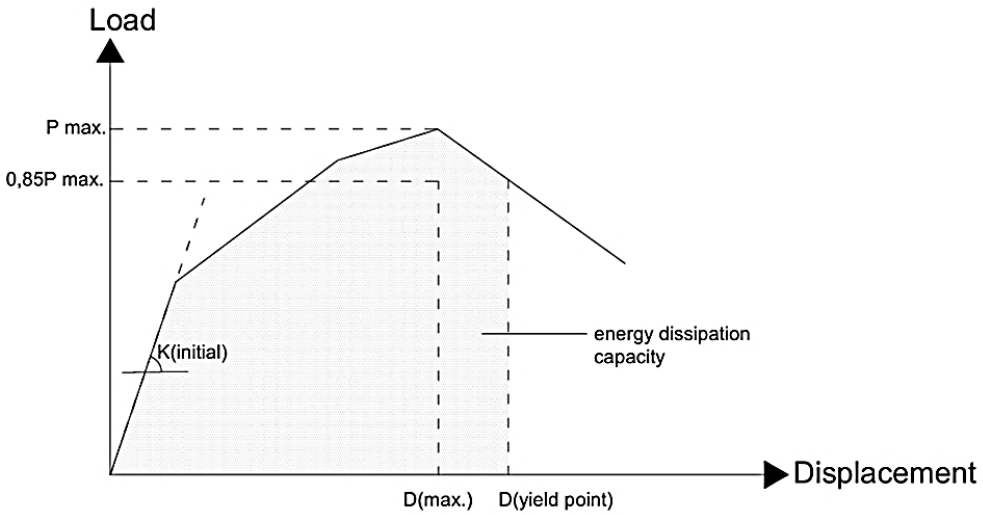

Figure 3. The approach used for calculating initial stiffness and energy dissipation capacity.

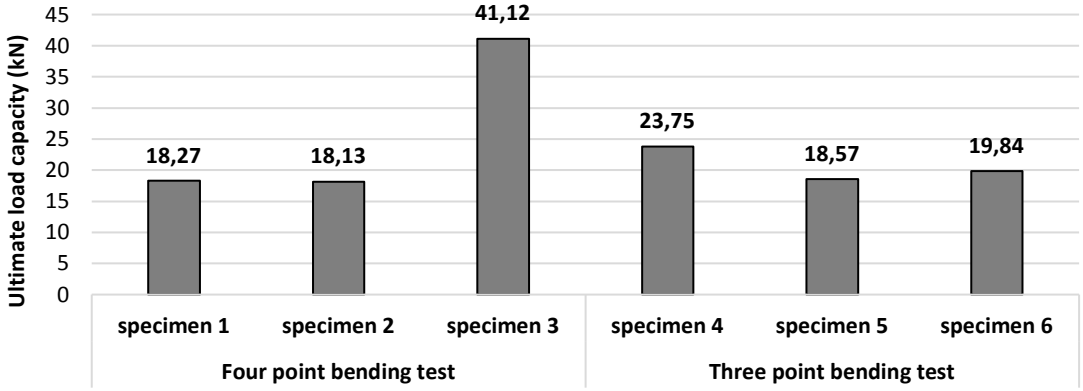

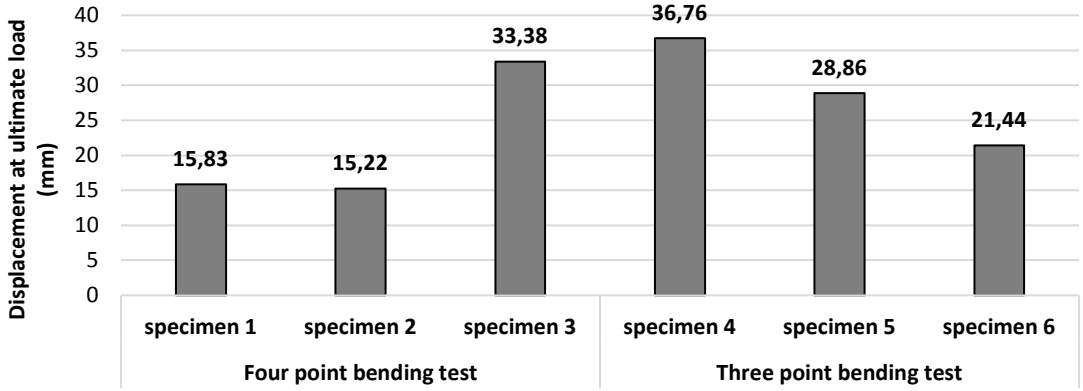

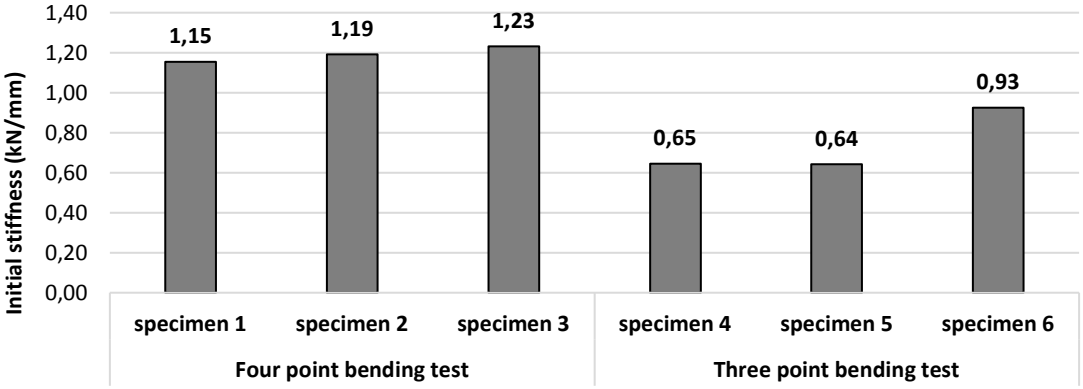

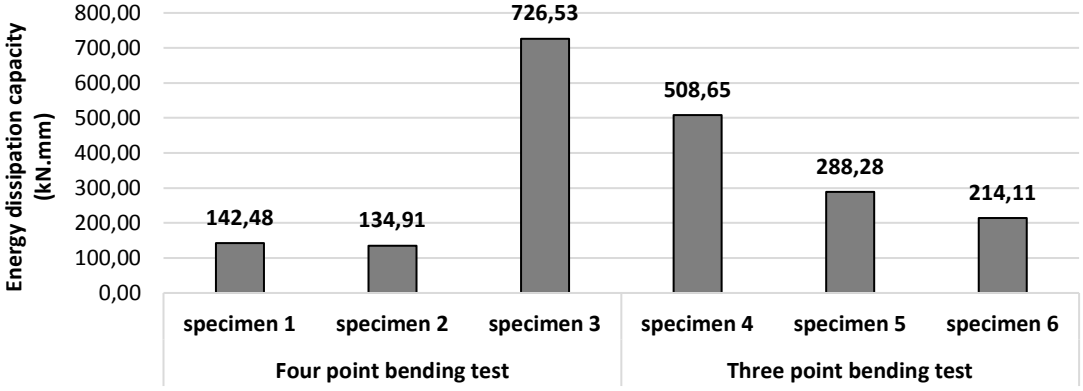

Figure 4. Graphs of the ultimate load capacity, displacement at ultimate load, initial stiffness and energy dissipation capacity values for test samples.

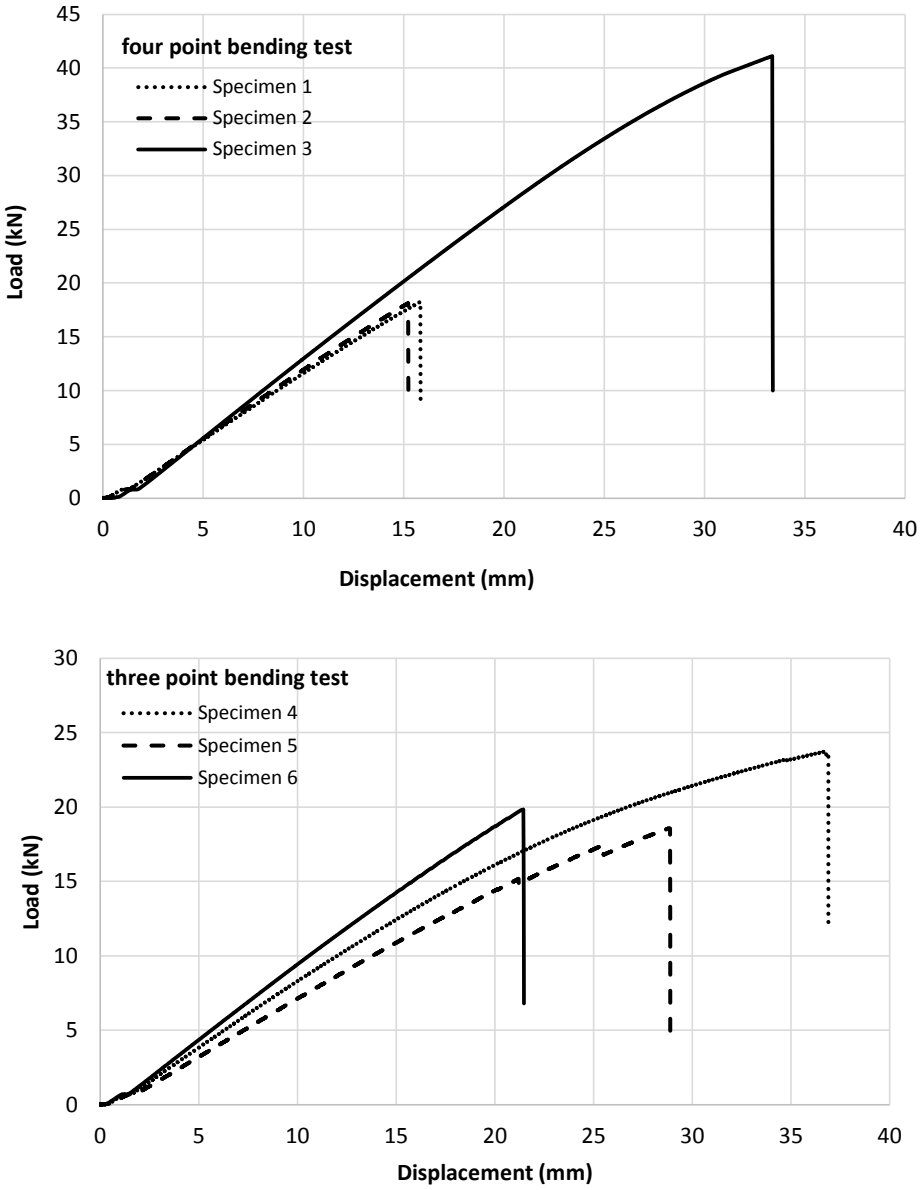

Figure 5. Load-displacement graphs of specimens.

Figure 6. Failure modes of specimens.

3.1. Loading Type Effect

When comparing the results of bending tests on glulam beams under different loading types, the ultimate load-bearing capacity of specimens tested using a three-point bending test was found to be higher than that of those tested with a four-point bending test, except for specimen 3. Notably, specimen 4, tested at the same loading rate (10 mm/min), showed approximately 30% greater ultimate load-bearing capacity than specimen 1, which underwent the four-point test. Similarly, for specimens 2 and 5, tested at 20 mm/min, specimen 5 exhibited about 3% higher ultimate load-bearing capacity compared to specimen 2, which was subjected to the four-point test. A similar result was found in a study by Hein and Brancheriau (2018). In their research on Eucalyptus specimens, they conducted both three-point and four-point bending tests and found that the average wood strength obtained from the three-point bending test (76.8 MPa) was higher than that obtained from the four-point bending test (73 MPa). They also emphasized that the volume of wood under maximum stress was greater in the four-point bending test, which led to longer exposure of the beam to the effects of internal cracks or defects at the moment of failure (Hein and Brancheriau, 2018).

The results obtained from the experimental study showed a contrasting outcome when comparing specimens 3 and 6 at the same loading rate (30 mm/min). Specimen 6, tested using the three-point bending method, exhibited approximately 52% lower results than specimen 3, which underwent the four-point bending test. These findings regarding the ultimate load-bearing capacities of the specimens were consistent for the displacement at ultimate load, maximum displacement, and energy dissipation capacity values as well.

In this context, when comparing specimens 1 and 4 at the same loading rate (10 mm/min), specimen 4, tested using the three-point bending method, showed approximately 132% significantly greater displacement at ultimate load compared to specimen 1, which was subjected to the four-point test. Similarly, at a loading rate of 20 mm/min, specimen 5 exhibited around 90% greater displacement at ultimate load compared to specimen 2. Conversely, for specimens 3 and 6 at the same loading rate (30 mm/min), specimen 6 showed approximately 35% lower displacement at ultimate load than specimen 3, which underwent the four-point bending test.

At the same loading rate (10 mm/min), specimen 4, tested using the three-point bending method, exhibited approximately 43% lower initial stiffness compared to specimen 1, which was subjected to the four-point bending test. Similarly, at a loading rate of 20 mm/min, specimen 5 showed around 46% lower initial stiffness compared to specimen 2. For specimens 3 and 6 at the same loading rate (30 mm/min), specimen 6, tested with the three-point method, resulted in approximately 24% lower initial stiffness than specimen 3, which underwent the four-point bending test.

At the same loading rate (10 mm/min), specimen 4, tested using the three-point bending method, demonstrated approximately four times greater energy dissipation capacity compared to specimen 1, which was subjected to the four-point bending test. Similarly, at a loading rate of 20 mm/min, specimen 5 exhibited more than twice the energy dissipation capacity of specimen 2. In contrast, for specimens 3 and 6 at the same loading rate (30 mm/min), specimen 6, tested with the three-point method, resulted in approximately one-third less energy dissipation capacity than specimen 3, which underwent the four-point bending test.

The experimental study revealed differences between the values obtained from three-point and four-point bending tests on glulam beams, with generally higher values recorded for specimens subjected to the three-point bending test compared to those tested using the four-point method at the same loading rates. This finding aligns with the results of Babiak et al. (2018), who conducted similar tests on spruce and oak wood specimens, noting discrepancies between the two testing methods. They suggested that these differences could be attributed to shear stresses (Babiak et al., 2018).

3.2. Loading Rate Effect

When comparing different loading rates in four-point bending tests conducted on glulam beams, specimen 1 reached an ultimate load capacity of 18.27 kN. Specimen 2, at a loading rate of 20 mm/min, resulted in approximately 0.7% lower maximum force than specimen 1. However, when specimen 3 was tested at a loading rate of 30 mm/min, it demonstrated a significantly higher ultimate load capacity, approximately 127% greater than that of specimen 2. Examining the displacements at ultimate load, specimen 1 exhibited a displacement of 15.83 mm. Specimen 2, under the same loading rate of 20 mm/min, showed about 4% less displacement at ultimate load compared to specimen 1. Conversely, specimen 3, tested at 30 mm/min, displayed approximately 119% greater displacement at ultimate load than specimen 2. In terms of initial stiffness, specimen 2 demonstrated about 3% greater initial stiffness compared to specimen 1, while specimen 3 showed approximately 3% greater initial stiffness than specimen 2. Regarding energy dissipation capacities, specimen 2 had an energy dissipation capacity about 5% lower than that of specimen 1, whereas specimen 3 exhibited a significantly higher energy dissipation capacity, nearly six times that of specimen 2.

In three-point bending tests conducted on glulam beams with varying loading rates, specimen 4 achieved an ultimate load capacity of 23.75 kN at a loading rate of 10 mm/min. Specimen 5, tested at 20 mm/min, exhibited approximately 22% lower ultimate load compared to specimen 4, while specimen 6, at 30 mm/min, showed about 7% higher maximum force than specimen 5. When comparing displacements at ultimate load, it was

observed that displacements gradually decreased with increasing loading rates. Specifically, specimen 5 had approximately 21% lower displacement than specimen 4, and specimen 6 exhibited about 25% lower displacement at ultimate load compared to specimen 5. In terms of initial stiffness, specimen 4 had a stiffness of 0.65 kN/mm, while specimen 5 was close at 0.64 kN/mm. However, specimen 6 demonstrated approximately 45% greater initial stiffness than specimen 5. Regarding energy dissipation capacities, the highest energy dissipation capacity was recorded for specimen 4 at 508.65 kN.mm. Specimen 5 had about 43% lower energy dissipation compared to specimen 4, while specimen 6 showed approximately 26% lower energy dissipation than specimen 5.

When evaluating the test results in terms of the effects of loading rates, both three-point and four-point bending tests showed significant impacts on the mechanical properties of the specimens. In this context, Gerhards (1977) noted that loading rate has a significant effect on wood. He indicated that loading speed is the most influential factor on the tensile strength perpendicular to the grain in dry wood, followed by the compressive strength parallel to the grain, as well as bending and shear strengths. He also mentioned that the effects of these last three properties do not differ significantly (Gerhards, 1977). In examining the effects of loading rates on glulam wood beams, both three-point and four-point bending tests revealed that as the loading rate increased from 10 mm/min to 20 mm/min, the ultimate load capacity of the specimens decreased. However, an increase from 20 mm/min to 30 mm/min resulted in a significant increase in ultimate load capacity, particularly for specimen 3. In the four-point bending test, the initial stiffness increased in parallel with the loading rate. In contrast, in the three-point bending test, the initial stiffness decreased when the loading rate increased from 10 mm/min to 20 mm/min, but increased again when the loading rate rose from 20 mm/min to 30 mm/min. The energy dissipation capacities also showed that in the four-point bending test, there was a decrease in energy dissipation at the loading rate of 20 mm/min, correlating with the ultimate load results. However, the highest value was obtained at the loading rate of 30 mm/min. In the three-point bending test, energy dissipation capacities gradually decreased with increasing loading rates.

When examining the experimental results based on the loading rate, it was found that, with the exception of the loading rate of 20 mm/min, an increase in loading rate led to an enhancement in the ultimate load, displacement at ultimate load, initial stiffness, and energy dissipation capacity in four-point bending tests. However, when assessing the three-point bending test results based on loading rates, no significant outcomes were observed regarding ultimate load, displacement at ultimate load, initial stiffness, and energy dissipation capacity with increasing loading rates. Similar findings were reported by Büyüksarı (2017), who conducted three-point bending tests on oak wood at different loading rates and noted that the loading rate had no statistically significant effect on the bending strength of oak. Nonetheless, it was mentioned that the strength and elastic modulus values generally decreased with a reduction in loading speed (Büyüksarı, 2017).

4. Conclusion

In the experimental study, test samples made from six sipo glulam wood elements were subjected to bending tests. The aim was to investigate and reveal the behavior of glulam samples under different loading types (four-point and three-point bending tests) and various loading rates (10 mm/min, 20 mm/min, and 30 mm/min). In this context, general load-displacement curves for the glulam samples were constructed based on the experimental data; from these graphs, the ultimate load capacity, displacement at ultimate load, initial stiffness, and energy dissipation capacities of the samples were determined. The results obtained from the study can be summarized as follows:

- There are differences observed in the values obtained from the three-point and four-point bending tests applied to the glulam beams.
- Generally, the samples subjected to the three-point bending test yielded higher values compared to those tested using the four-point bending test at the same loading rates. However, this result was not applicable to the sample tested with the four-point bending method at a loading rate of 30 mm/min.
- The different loading rates (10 mm/min, 20 mm/min, and 30 mm/min) applied to the glulam beams affected the results obtained from both the three-point and four-point bending tests.
- In the four-point bending test, an increase in the loading rate led to enhancements in the ultimate load, displacement at ultimate load, initial stiffness, and energy dissipation capacity of the samples. However, this result was not applicable at the loading rate of 20 mm/min, where decreases were observed in the ultimate load, displacement at ultimate load, and energy dissipation capacity.
- In the three-point bending test, no significant results were obtained regarding the ultimate load, displacement at ultimate load, initial stiffness, and energy dissipation capacity with increasing loading rates. It was noted that the displacement at ultimate load and energy dissipation capacity values decreased as the loading rate increased.
- In both the four-point and three-point bending tests, a significant decrease in the values of the samples was observed at the loading rate of 20 mm/min.
- In the case of the four-point bending test conducted at a loading rate of 30 mm/min, the values were found to be at their highest level.

Author Contributions

The percentages of the author contributions are presented below. The author reviewed and approved the final version of the manuscript.

	M.A.K.A
C	100
D	100
S	100
DCP	100
DAI	100
L	100
W	100
CR	100
SR	100
PM	100
FA	100

C=Concept, D= design, S= supervision, DCP= data collection and/or processing, DAI= data analysis and/or interpretation, L= literature search, W= writing, CR= critical review, SR= submission and revision, PM= project management, FA= funding acquisition.

Conflict of Interest

The author declared that there is no conflict of interest.

Ethical Consideration

Ethics committee approval was not required for this study because of there was no study on animals or humans.

Acknowledgements

The author would like to thank the "Department of Civil Engineering at Ankara University" for the use of the "Structural Mechanics Laboratory".

References

Babiak M, Gaff M, Sikora A, Hysek Š. 2018. Modulus of elasticity in three-and four-point bending of wood. Compos Struct, 204: 454-465.

Brancheriau L, Bailleres H, Guitard D. 2002. Comparison between modulus of elasticity values calculated using 3 and 4 point bending tests on wooden samples. Wood Sci Technol, 36(5): 367-383.

Büyüksari Ü. 2017. Effect of loading rate on mechanical properties of micro-sized oak wood. Maderas, 19(2): 163-172.

Das AK, Islam MN, Ghosh CK, Ghosh RK. 2023. Physical and mechanical properties of Albizia procera glulam beam. Heliyon, 9(8).

Gérard J, Guibal D, Paradis S, Cerre JC. 2017. Tropical timber atlas: technological characteristics and uses. Éditions Quæ. RD 10 78026 Versailles Cedex, Paris, France, pp: 834-836

Gerhards CC. 1977. Effect of duration and rate of loading on strength of wood and wood-based materials, USDA Forest Service Research Paper, U.S. Department of Agriculture Forest Service Forest Products Laboratory Madison, Wis, USA, pp: 1-24.

Ghoroubi R, Mercimek Ö, Sakin S, Anil Ö. 2022. Experimental investigation of bonding behavior of anchoraged timber-to-timber joint. Arch Civ Mech Eng, 22: 1-16.

He M, Wang Y, Li Z, Zhou L, Tong Y, Sun X. 2022. An experimental and analytical study on the bending performance of CFRP-reinforced glulam beams. Front Mater, 8: 802249.

Hein PRG, Brancheriau L. 2018. Comparison between three-point and four-point flexural tests to determine wood strength of Eucalyptus specimens. Maderas, 20(3): 333-342.

Issa CA, Kmeid Z. 2005. Advanced wood engineering: glulam beams. Constr Build Mater, 19(2): 99-106.

İşleyen ÜK, Ghoroubi R, Mercimek Ö, Anıl Ö, Erdem RT. 2023. Investigation of impact behavior of glulam beam strengthened with CFRP. Struct, 51: 196-214.

İşleyen ÜK, Ghoroubi R, Mercimek Ö, Anil Ö, Erdem RT. 2021a. Behavior of glulam timber beam strengthened with carbon fiber reinforced polymer strip for flexural loading. J Reinf Plast Compos, 40(17-18): 665-685.

İşleyen ÜK, Ghoroubi R, Mercimek Ö, Anıl Ö, Togay A, Erdem RT. 2021b. Effect of anchorage number and CFRP strips length on behavior of strengthened glulam timber beam for flexural loading. Adv Struct Eng, 24(9): 1869-1882.

Li H, Ren Y, Zuo T, Xu X, Wang Y, Tian P. 2024. Experimental study of flexural behavior of glulam Douglas Fir beams spliced with engineered bamboo cover plates and inclined self-tapping screws. Struct, 65: 106658.

Mei L, Ren J, Lin X, Wu M, Guo N, Yang W, Sheng Y. 2024. Analytical model for prestressed glulam beams reinforced with unbonded steel bars. Eng Struct, 307: 117862.

Mercimek Ö, Ghoroubi R, Akkaya ST, Türer A, Anıl Ö, İşleyen, ÜK. 2024. Flexural behavior of finger joint connected glulam wooden beams strengthened with CFRP strips. Struct 66: 106853.

Stark NM, Cai Z, Carll C. 2010. Wood-based composite materials panel products, glued-laminated timber, structural composite lumber, and wood–nonwood composite materials. In: Ross RJ, editor. Wood handbook: wood as an engineering material. Forest Products Laboratory, United States Department of Agriculture Forest Service Madison, Wisconsin, USA, pp: (11-1)-(11-26).

Uzel M, Togay A, Anil Ö, Söğütlü C. 2018. Experimental investigation of flexural behavior of glulam beams reinforced with different bonding surface materials. Constr. Build Mater, 158: 149-163.

Wang Y, He M, Li Z. 2024. Flexural behavior of glulam beams reinforced by bonded prestressing tendons. Eng Struct, 315:118436.

Wang T, Wang Y, Ringaby J, Crocetti R, Wålinder M, Blomqvist L. 2024. Glulam beams adhesively bonded by birch plywood plates in moment-resisting beam-to-beam connections. Eng Struct, 302:117471.

Yang H, Liu W, Lu W, Zhu S, Geng Q. 2016. Flexural behavior of FRP and steel reinforced glulam beams: Experimental and theoretical evaluation. Constr Build Mater, 106: 550-563.

Yoshihara H. 2013. Comparison of results obtained by static 3- and 4-point bending and flexural vibration tests on solid wood, MDF, and 5-plywood. HF, 67(8): 941-948.

Zhao J, Liu H, Chen Z, Zhao S, Yang S, He F. 2023. Investigation on the mechanical behavior of glulam beam string. Struct, 52: 582-597.

Zhang X, Zhang Y, Xie X. 2023. Experimental and analytical investigation of the flexural behaviour of stiffened hollow glulam beams reinforced with fibre reinforced polymer. Struct, 50: 810-822.